Colloid Polym Sci 274:290–294 (1996)

SHORT COMMUNICATION

K. Kandori
T. Imazato
A. Yasukawa
T. Ishikawa

Texture of spherical aluminum phosphate particles

Received: 5 July 1995
Accepted: 26 October 1995

Dr. K. Kandori (✉) · T. Imazato
A. Yasukawa · T. Ishikawa
School of Chemistry
Osaka University of Education
Asahigaoka 4-698-1, Kashiwara-shi
Osaka 582, Japan

Abstract Spherical aluminum phosphate particles with a mean particle diameter of 477 ± 16 nm, produced from aging of a solution containing $Al(NO_3)_3$, Na_2HPO_4 and HNO_3 at 100 °C for 19 h in 20-cm^3 Teflon-lined screw-capped Pyrex test tube without agitation, were characterized by various means. It was revealed from x-ray diffraction measurement and transmission electron microscope observation that amorphous particles are formed by agglomeration of small primary particles. The particles exhibited a high selective adsorption of H_2O though they adsorbed small amount of N_2 and CO_2. This characteristic phenomenon was explained by rehydration of Al^{3+} ions by H_2O molecules that were penetrated into the particles.

Key words Spherical metal phosphate – aluminum phosphate – texture – characterization – selective adsorption of H_2O

Introduction

Aluminum phosphate is of interest in adsorbents, catalyst carriers, and possibly as catalysts [1, 2]. Some aluminum phosphate particles are known to show a high catalytic activity and a stronger surface acidity than silica–alumina cracking catalysts [1]. On the other hand, Wilson et al. have reported that aluminum phosphate can be produced as a porous crystalline material as well as zeolite [3, 4]. This aluminum phosphate molecular sieve ($AlPO_4$-*n*) can be endowed with Brønsted acidity by isomorphous substitution of hetero atoms into their frameworks [5–7]. Recently, AlPO-18 substituted with silicon and divalent metal (designated as SAPO-18 and MAPO-18, respectively) was synthesized and it was claimed that these molecular sieves are excellent solid acid catalysts for methanol conversion to light alkanes [8, 9]. However, all these molecular sieve particles are not uniform either in shape and size. If we can prepare the particles with uniform shape and size, these characteristic properties would be more emphasized by the uniformity of the surface and inner structures of these particles, which permits us to design many high efficient products. Matijević and his collaborators have reported the preparation and properties of various uniform metal phosphate particles [10–15]. Recently, we have investigated the inner structure of these uniform particles and found that cobalt phosphate particles possess a thermally unstable layer structure which exhibits a high selective adsorption of H_2O by their molecular sieve effects [16], while nickel phosphate particles are agglomerates of the fine primary particles which exhibit a high mesoporosity [17]. This study was conducted as a continuation of previous studies to investigate the surface and inner structures of spherical aluminum phosphate particles.

Experimental

Aluminum phosphate particles were prepared by aging a solution of $Al(NO_3)_3$ ($3.16 \times 10^{-2} \sim 7.95 \times 10^{-2}$ mol/dm^3), Na_2HPO_4 ($3.16 \times 10^{-2} \sim 7.95 \times 10^{-2}$ mol/dm^3) and

HNO_3 (0.1 mol/dm^3) in a 20-cm^3 Teflon-lined screw-capped Pyrex test tube with an air turbulent circulation oven for various aging periods varying from 1 to 48 h at 100 °C [10]. The resulting particles were washed thoroughly by distilled water on Millipore filter (220 nm) and finally dried **in vacuo** at room temperature for 16 h. The pH change of the solutions during aging was recorded at room temperature. All the chemicals used were a guaranteed reagent grade from Wako Pure Chemical Industries Ltd. and were used without further purification.

The resulting particles were characterized by transmission electron microscope (TEM), simultaneous thermogravimetry and differential thermal analysis (TG-DTA), *in situ* Fourier transform infrared spectrophotometry (FTIR), x-ray powder diffraction measurement (XRD), zeta potential measurement and adsorptions of N_2 at liquid N_2 temperature, H_2O at 25 °C and CO_2 at 10 °C as described elsewhere [16–18]. Al and P contents of the particles were assayed respectively with an inductively coupled plasma spectroscopy (ICP) and a molybdenum blue method in HCl solution.

Results and discussion

It was found from preliminary studies that spherical aluminum phosphate particles can be prepared at 3.98×10^{-2} mol/dm^3 $Al(NO_3)_3$ and 3.98×10^{-2} mol/dm^3 Na_2HPO_4. The particle size increased with progressing aging and became constant after aging for 19 h in this condition. TEM photograph of the particles, formed after aging for 19 h and employed for characterization throughout in this study, is displayed in Fig. 1A. The pH of the solution decreased slightly from 2.02 to 1.90 with aging of the solution. The acidic condition with HNO_3 prevented the hydrolysis of Al^{3+} ions to $Al(OH)_n^{(3-n)+}$. In this acidic condition, phosphoric acid could dissociate to produce HPO_4^{2-} and/or $H_2PO_4^-$ ions, leading to a decrease of solution pH as described above. Figure 1B displays the TEM picture of the particles produced after aging for 2 h. It is obviously recognized that the particles grew via the agglomeration of small primary particles, similar to the case of spherical cadmium, nickel and manganese phosphate particles reported by several investigators [14–16]. The large void spaces visualized on the TEM picture of the samples (Fig. 1C), exposed to a high electron beam irradiation during TEM observation, may further suggest the existence of openings between the agglomerated particles. The diameter of the spherical aluminum phosphate particles produced by aging for 19 h (Fig. 1A) was distributed from 100 to 800 nm and the mean particle diameter was 477 ± 16 nm. Compared to the cobalt and nickel phosphate particles reported in our previous papers [16, 17],

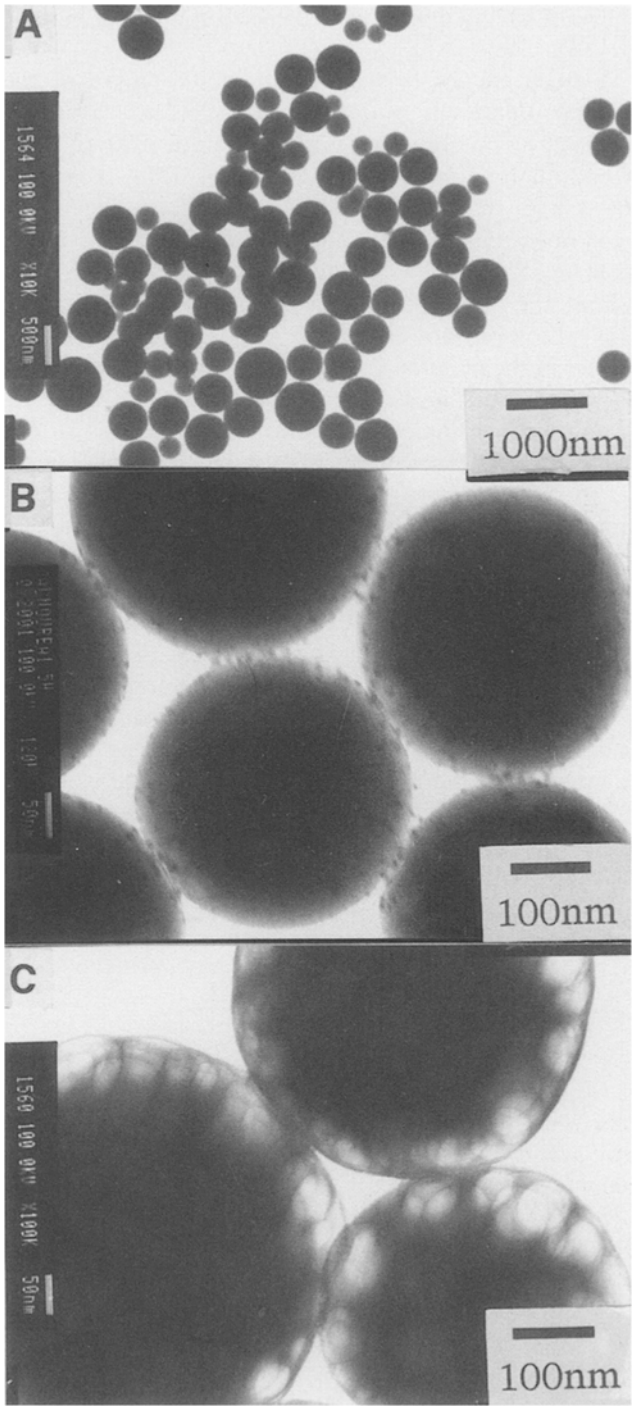

Fig. 1 Transmission electron microphotographs of aluminum phosphate particles produced from the aging of a mixed solution of $[Al(NO_3)_3] = 3.98 \times 10^{-2}$ mol/dm^3, $[Na_2HPO_4] = 3.98 \times 10^{-2}$mol/dm^3 and $[HNO_3] = 0.1$ mol/dm^3 at 100 °C for 19 h (A) and 2 h (B). (C) Sample A after exposed to a high electron beam

the uniformity in size of aluminum phosphate particles produced in this study is poor. This would be because the aluminum phosphate particles were prepared with no

surfactant having a pronounced effect on unifying particle size [18].

A steep weight loss appeared in TG curve of the spherical aluminum phosphate particles up to 200 °C followed by a monotonous weight loss until 1000 °C. Since an endothermic peak is observed in DTA curve at 100 ~ 150 °C, this weight loss can be ascribed to the release of adsorbed and/or coordinated water. The total weight loss from 25 to 1000 °C was 21.5%. The molar ratio of Al to P in the particles was 1.04. These results offer the chemical composition as $AlPO_4 \cdot 1.9H_2O$, though the state of water in the material is uncertain due to its low crystallinity as will be described later. The large extent of adsorbed and/or coordinated water on the material was further detected by FTIR measurement as shown in Fig. 2. The IR spectra in Fig. 2 were measured *in situ* at room temperature after evacuating at various temperatures. A strong broad band appears at 3500 ~ 3550 cm^{-1}. The intensity of this band decreases with elevating the evacuating temperature, but the band remains even at 400 °C. Comparing to the results of TG, this band can be assigned to the stretching mode of OH groups of H_2O molecules coordinated to Al^{3+} ions and/or strongly adsorbed to the particles.

The zeta potential was inverted from positive to negative with increasing pH and an isoelectric point could be determined at pH 6, implying that the particle surface is virtually neutral. The XRD measurement using CuKα radiation revealed that freshly prepared aluminum phosphate particles are amorphous. However, four sharp peaks appeared at 2θ of 20.3, 21.4, 22.8 and 35.5° after treating at 1000 °C for 2 h in air. These peaks are consistent with the literature values of $AlPO_4$ (tridymite) [19], while other characteristic peaks reported in the literature were not detected. Therefore, the detailed identification is impossible at present.

All the N_2 adsorption isotherms on the particles outgassed at various temperatures belonged to Type II in the BDDT classification [20]. Compared to a drastic change on the amounts of adsorbed H_2O with pretreatment temperature as shown in Fig. 3, the variation of N_2 adsorption is anticipated to be very small. To determine the specific surface area of the particles, the BET equation was

Fig. 2 IR spectrum of aluminum phosphate particles as shown in Fig. 1A after being pretreated at various temperatures in vacuo. (a) 25°, (b) 50°, (c) 100°, (d) 200°, (e) 300° and (f) 400 °C

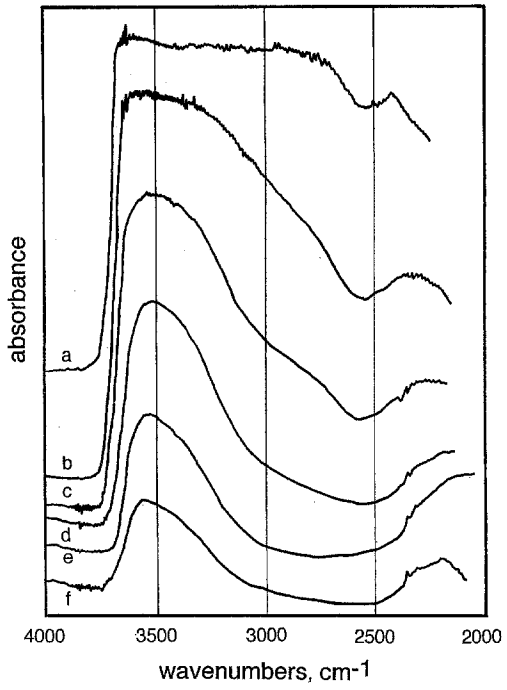

Fig. 3 Adsorption isotherms of H_2O on aluminum phosphate particles as shown in Fig. 1A pretreated at various temperatures in vacuo (a) and in air (b). (a) (□) 25°, (○) 37.5°, (△) 50°, ( ) 75°, (◆) 100°, (⊕) 150°, (▽) 200°, (◪) 300°, (⊠) 400 °C; (b) (□) 200°, (▽) 400°, (○) 600°, (△) 800°, ( ) 1000 °C. The filled square represents the desorption isotherm of the sample pretreated at 25 °C

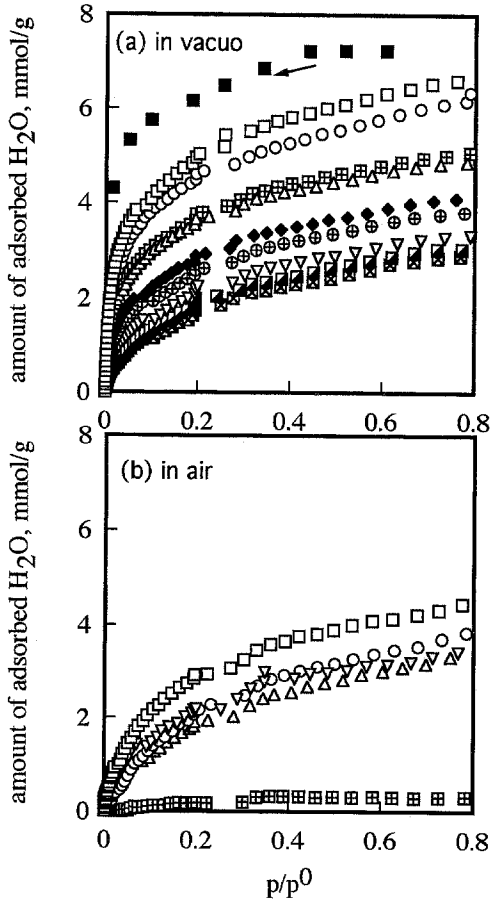

applied to these N_2 adsorption isotherms between p/p^0 from 0.05 to 0.35. The C constant of the BET equation obtained from the analysis ranged from 10 to 49 and good linear BET plots were attained. The specific surface area obtained by using a cross-sectional area of N_2 molecule of 0.162 nm^2 ranged from 9 to 15 m^2/g, being only a few times larger than the specific surface area of 4.9 m^2/g calculated from the mean particle diameter (477 nm) assuming the density of the particles as 2.57 g/cm^3. This result means that the particles are nearly nonporous for N_2 molecule.

On the other hand, the particles adsorbed large amounts of H_2O molecules, especially pretreated at low temperatures, as depicted in Fig. 3. The monolayer adsorption capacity of H_2O (n_w) was evaluated by fitting these isotherms to the BET equation as same as the N_2 adsorption. The C constant of the BET equation ranged from 36 to 75 and gave good linear BET plots except for the particles pretreated at 1000 °C for 2 h in air showing a low C constant of 3. Figure 4 plots n_w in molecules/nm^2 units based on N_2 surface area against pretreatment temperature. The theoretical n_w value on the nonporous particle is 9.3 molecules/nm^2 estimated from the cross-sectional area of H_2O molecule (0.108 nm^2) as is depicted by a dashed line in Fig. 4. It is understandable from this figure that the particles pretreated below 200 °C show rather large n_w, suggesting the particles possess a high adsorption selectivity of H_2O. The desorption isotherm of H_2O for the materials outgassed at 25 °C (full square in Fig. 3) indicates that the isotherm of H_2O possesses a large hysteresis loop that does not close until the relative pressure reaches zero. This isotherm closed at zero of p/p^0 on prolonged evacuating, revealing that H_2O is reversibly adsorbed.

Besides the adsorption measurements of N_2 and H_2O, we further measured the adsorption isotherms of CO_2 at 10 °C on the particles pretreated at 25 °C to examine the polarity of the particle surface. The linear CO_2 molecule has a higher quadrupole moment ($1.03 \sim 1.13 \times 10^{-37}$ Cm) than that of N_2 and chemisorption can be excluded from consideration [21]. However, the Henry-type isotherm was obtained, in which the adsorbed amount of CO_2 was proportional to the pressure up to 1.33×10^5 Pa ($p/p^0 = 2.96 \times 10^{-2}$), signifying a low affinity of CO_2 to the material. This fact indicates that the polar groups or ions are absent on the particle surface, coinciding with a surface neutrality ascertained by the zeta potential measurement. It can be presumed from the above result that the unique high adsorption selectivity of H_2O is due to rehydration of the particles by adsorbed H_2O as same as the case of chromium oxide gels prepared from chromium nitrate solution utilizing the slow hydrolysis of urea [22]. The hydrogels, freshly formed from highly hydrated Al^{3+} ions, are usually poorly ordered and retain considerable amounts of hydrated H_2O. These hydrated H_2O molecules are removed by outgassing without an appreciable structural change or collapse of the solid framework. The cavities formed near the cations by outgassing serve for H_2O adsorption but not for N_2 and CO_2 ones. Thus, the rehydration of Al^{3+} ions by H_2O penetrated in the cavities may take place due to the coordination of adsorbed H_2O to Al^{3+} ions. The large hysteresis loop of the adsorption–desorption isotherm of H_2O (Fig. 3) strongly supports a penetration hypothesis. Of course, a possibility of molecular sieve effect of ultramicropores that are accessible to H_2O molecules but not to N_2 and CO_2 ones, as reported in our previous papers on cobalt and nickel phosphates particles [16, 18], still remains. Therefore, the detailed study in progress may throw more light on the mechanism of the selective adsorption of H_2O.

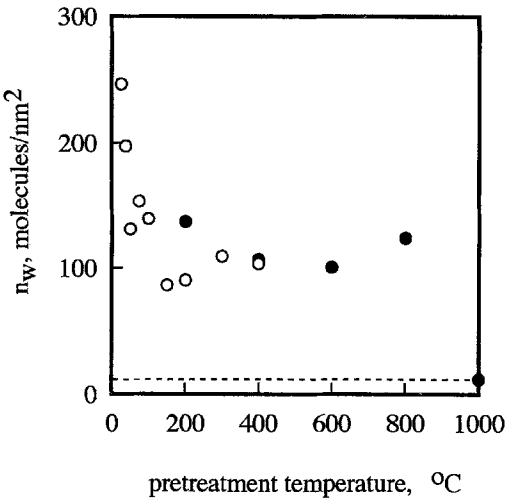

Fig. 4 Plots of n_w as a function of pretreatment temperature. The filled symbols represent the samples pretreated in air

Acknowledgement The authors thank Mr. Masao Fukusumi of Osaka Municipal Technical Research Institute for help with the TEM observations. This work has been supported in part by the Grant-in-Aid for Scientific Research (C) of the Ministry of Education, Science, Sports and Culture, and Nippon Sheet Glass Foundation for Materials Science and Technology.

References

1. Kearby KK (1967) US Patent 3,342,750
2. Veltman PL (1942) US Patent 2,301,013
3. Wilson ST, Lok BM, Flanigen EM (1982) US Patent 4,310,440
4. Wilson ST, Lok BM, Messina CA, Cannan TR, Flanigen EM (1982) J Am Chem Soc 104:1146
5. Lok BM, Messina CA, Patton RL, Gajek RT, Cannan TR, Flanigen EM (1984) J Am Chem Soc 106:6092
6. Flanigen EM, Lok BM, Patton RL, Wilson ST (1986) Pure Appl Chem 58:1351
7. Flanigen EM, Patton RL, Wilson ST (1988) Stud Surf Sci Catal 37:13
8. Chen J, Thomas JM, Townsend RP, Lok CM (1993) UK Patent 9318644.3
9. Chen J, Thomas JM (1994) J Chem Soc Chem Commun 603
10. Katsanis EP, Matijević E (1982) Colloids Surf 5:43
11. Wilhelmy RB, Patel RC, Matijević E (1985) Inorg Chem 24:3290
12. Ishikawa T, Matijević E (1988) J Colloid Interface Sci 123:122
13. Wilhelmy RB, Matijević E (1987) Colloids Surf 22:111
14. Springsteen LL, Matijević E (1989) Colloid Polym Sci 267:1007
15. Morales G, Clemente RR, Matijević E (1992) J Colloid Interface Sci 151:555
16. Kandori K, Toshioka M, Nakashima H, Ishikawa T (1993) Langmuir 9:1031
17. Kandori K, Nakashima H, Ishikawa T (1993) J Colloid Interface Sci 160:499
18. Kandori K, Matsuda E, Yasukawa A, Ishikawa T (1995) Shikizai 68:75
19. JCPDS file no. 15-254
20. Brunauer S, Deming LS, Deming WE, Teller E (1940) J Am Chem Soc 62:1723
21. Gregg SJ, Sing KSW (1982) "Adsorption, Surface Area and Porosity", 2nd ed.; Academic Press, London
22. Baker FS, Sing KSW, Stryker LJ (1970) Chemistry and Industry 30:718